THE FASEB JOURNAL • RESEARCH • www.fasebj.org

The role of raptor in the mechanical load-induced regulation of mTOR signaling, protein synthesis, and skeletal muscle hypertrophy

Jae-Sung You,[*,†,1] Rachel M. McNally,[*,†,1] Brittany L. Jacobs,[*,†,1] Rachel E. Privett,[*,†] David M. Gundermann,[*,†] Kuan-Hung Lin,[*,†] Nate D. Steinert,[*,†] Craig A. Goodman,[*,†,‡,§] and Troy A. Hornberger[*,†,2]

[*]Department of Comparative Biosciences and [†]School of Veterinary Medicine, University of Wisconsin–Madison, Madison, Wisconsin, USA; [‡]Institute of Health and Sport, Victoria University, Melbourne, Victoria, Australia; and [§]Australian Institute for Musculoskeletal Science, Victoria University, St. Albans, Victoria, Australia

ABSTRACT: It is well known that an increase in mechanical loading can induce skeletal muscle hypertrophy, and a long standing model in the field indicates that mechanical loads induce hypertrophy *via* a mechanism that requires signaling through the mechanistic target of rapamycin complex 1 (mTORC1). Specifically, it has been widely proposed that mechanical loads activate signaling through mTORC1 and that this, in turn, promotes an increase in the rate of protein synthesis and the subsequent hypertrophic response. However, this model is based on a number of important assumptions that have not been rigorously tested. In this study, we created skeletal muscle specific and inducible raptor knockout mice to eliminate signaling by mTORC1, and with these mice we were able to directly demonstrate that mechanical stimuli can activate signaling by mTORC1, and that mTORC1 is necessary for mechanical load-induced hypertrophy. Surprisingly, however, we also obtained multiple lines of evidence that indicate that mTORC1 is not required for a mechanical load-induced increase in the rate of protein synthesis. This observation highlights an important shortcoming in our understanding of how mechanical loads induce hypertrophy and illustrates that additional mTORC1-independent mechanisms play a critical role in this process.—You, J.-S., McNally, R. M., Jacobs, B. L., Privett, R. E., Gundermann, D. M., Lin, K.-H., Steinert, N. D., Goodman, C. A., Hornberger, T. A. The role of raptor in the mechanical load-induced regulation of mTOR signaling, protein synthesis, and skeletal muscle hypertrophy. FASEB J. 33, 4021–4034 (2019). www.fasebj.org

KEY WORDS: mTORC1 · rapamycin · mechanotransduction · exercise · growth

Comprising ~45% of the body's mass, skeletal muscles are not only the motors that drive locomotion, but they also play a critical role in breathing, whole body metabolism, and maintaining a high quality of life (1). Indeed, both sedentary and active adults will lose 30–40% of their muscle mass by the age of 80, and this loss in muscle mass is associated with disability, loss of independence, and an increased risk of morbidity and mortality, as well as an estimated $18.5 billion in annual healthcare costs in the United States alone (1–3). Thus, the development of therapies that can restore, maintain, and/or increase muscle mass is of great clinical and fiscal significance. However, to develop such therapies, we will first need to establish a comprehensive understanding of the molecular mechanisms that regulate skeletal muscle mass.

Previous studies have shown that skeletal muscle mass can be regulated by a variety of different stimuli, with one of the most widely recognized stimuli being mechanical loading (4, 5). Despite the well-established role that mechanical loads play in the control of muscle mass, our understanding of the molecular mechanisms *via* which mechanical loads induce alterations in muscle mass remains ill-defined. Nevertheless, advancements are being made. For instance, work from numerous laboratories has shown that signaling through a rapamycin-sensitive mechanism plays a central role in the pathways through which mechanical loads induce a hypertrophic response

ABBREVIATIONS: 4EBP1, eukaryotic translation initiation factor 4E-binding protein 1; EDL, extensor digitorum longus; eMHC, embryonic myosin heavy chain; HSA, human skeletal actin; *iRAmKO*$^{+}$, inducible skeletal muscle raptor knockout positive; *iRAmKO*$^{-}$, inducible skeletal muscle raptor knockout negative; LAMP2, lysosome associated membrane protein 2; LEL, late endosome/lysosome; MCM, mutated estrogen receptor flanked cre-recombinase; MIC, maximal-intensity contraction; mTOR, mechanistic/mammalian target of rapamycin; mTORC1, mechanistic/mammalian target of rapamycin complex 1; p70, 70kDa ribosomal S6 kinase; RAmKO, skeletal muscle raptor knockout; RSmTOR, rapamycin-sensitive mTOR; S6, ribosomal S6 protein; TA, tibialis anterior

[1] These authors contributed equally to this work.

[2] Correspondence: University of Wisconsin Madison School of Veterinary Medicine, 2015 Linden Dr., Madison, WI 53706, USA. E-mail: troy.hornberger@wisc.edu

doi: 10.1096/fj.201801653RR

This article includes supplemental data. Please visit *http://www.fasebj.org* to obtain this information.

(6–9). Moreover, it has been demonstrated that a serine/threonine kinase called the mechanistic (or mammalian) target of rapamycin (mTOR) is the rapamycin-sensitive element that confers mechanical load-induced hypertrophy, and that the role of mTOR in this process requires its kinase activity (7). In other words, a strong body of evidence indicates that mechanical load-induced hypertrophy requires a rapamycin-sensitive pool of mTOR-dependent signaling events [referred to as rapamycin-sensitive mTOR (RSmTOR)-dependent from here forward].

mTOR can be found in at least 2 multiprotein signaling complexes called mTORC1 and mTORC2. The defining component of mTORC1 is a protein called raptor, whereas the defining component of mTORC2 is a protein called rictor (10). Previous studies have shown that a subset of mTORC1-dependent, but not mTORC2-dependent, signaling events are highly sensitive to inhibition by rapamycin (10–12). For this reason, it has been widely assumed that mTORC1 is responsible for the RSmTOR-dependent signaling events that control mechanical load-induced hypertrophy (13, 14). However, a growing body of evidence has raised concerns about this assumption. For instance, both rapamycin administration and the knockdown of mTOR can potently inhibit the translation of 5′TOP mRNAs; yet, knocking out raptor/mTORC1 only slightly impairs the translation of these mRNAs (15). Previous studies have also revealed that myogenesis proceeds through a RSmTOR-dependent mechanism that does not require raptor/mTORC1 (16). Finally, it has been shown that, even in the absence of raptor, mTOR can still induce changes in the phosphorylation of classic mTORC1 substrates and that this effect is mediated *via* a rapamycin-sensitive mechanism (17, 18). Simply put, an emerging body of literature suggests that there may be a pool of RSmTOR-dependent signaling events that do not involve signaling by the canonical mTORC1. Whether mechanical loads promote an increase in muscle mass by signaling through this noncanonical pool of RSmTOR, and/or mTORC1, has not been clearly resolved. For instance, in an effort to determine whether raptor/mTORC1 is necessary for mechanical load-induced hypertrophy, Bentzinger *et al.* performed a study with 90-d-old constitutive skeletal muscle raptor knockout (RAmKO) mice, in which the plantaris muscles of these knockout mice were subjected to mechanical overload *via* surgical ablation of the synergist muscles (*i.e.*, the synergist ablation model) (19). The results indicated that, unlike the muscles from control mice, the muscles of RAmKO mice did not undergo a hypertrophic response, and thus it was concluded that raptor/mTORC1 is required for mechanical load-induced hypertrophy (19). However, the interpretation of the results from this study is confounded by a number of traits that are inherent to the RAmKO mice. For instance, skeletal muscles from 90-d-old RAmKO mice present with a significant reduction in mitochondrial content along with numerous signs of dystrophy, including a decrease in mass and fiber size, an increase in centrally located nuclei, and the presence of central core-like structures within the muscle fibers (20). Moreover, it has been shown that the daily voluntary activity of 90-d-old RAmKO mice is dramatically reduced when compared with control mice (20). The reduction in voluntary activity is particularly concerning because, in the synergist ablation model, the amount of mechanical overload that is placed on the muscles is directly proportional to the animals' level of activity. Hence, the lack of a hypertrophic response in the muscles of RAmKO mice might simply have been due to animals not placing enough mechanical overload on the muscles to induce a hypertrophic response. Because of this limitation, and the other traits that are inherent to RAmKO mice, the role of raptor/mTORC1 in mechanical load-induced hypertrophy remains unsettled.

In this study, we have attempted to address the limitations of the RAmKO mice by creating skeletal muscle specific and inducible raptor knockout mice. We then used these mice, along with various models of mechanical loading, to determine whether raptor/mTORC1 is responsible for the RSmTOR-dependent signaling events that are induced by mechanical stimuli, and ultimately, whether raptor/mTORC1 is necessary for mechanical load-induced hypertrophy.

MATERIALS AND METHODS

Animals

Skeletal muscle specific and tamoxifen inducible raptor knockout mice were created by crossing female mice homozygous for exon 6 of raptor flanked by *loxP* sites (The Jackson Laboratory, Bar Harbor, ME, USA) with male mice hemizygous for human skeletal actin (HSA) promoter driven expression of a Cre recombinase that is flanked by mutated estrogen receptors (HSA-MCM) (21). The HSA-MCM hemizygotic mice were a generous gift from K. Esser (University of Florida, Gainsville, FL, USA) and have been previously described (22). Offspring were crossed until male mice homozygous for floxed raptor and hemizygous for HSA-MCM alleles [inducible RAmKO positive ($iRAmKO^{+}$)] were obtained. Male mice that were homozygous for floxed raptor, but did not contain the HSA-MCM allele, were used for the control condition ($iRAmKO^{-}$). In all cases, genotypes were confirmed with tail snips by PCR.

Wild-type C57BL6 and FVB mice were obtained from The Jackson Laboratory. FVB mice with HSA driven expression of a rapamycin-resistant mutant of mTOR (RR-mTOR) have been previously described (7). These mice were bred with wild-type FVB mice to produce offspring containing hemizygotic expression of RR-mTOR. The offspring that did not express RR-mTOR were used for the control condition.

All animals were housed in a room maintained with a 12-h light/dark cycle and received food and water *ad libitum*. Experimental procedures were performed on male mice that were 6–12 wk of age. Before all surgical procedures, mice were anesthetized with isoflurane and then, immediately following completion of a surgery, the mice were given an intraperitoneal injection of 0.05 μg/g of buprenorphine. After tissue extraction, the mice were euthanized by cervical dislocation. The Institutional Animal Care and Use Committee at the University of Wisconsin–Madison approved all of the methods used in this study.

Tamoxifen injections

Tamoxifen was purchased from MilliporeSigma (Burlington, MA, USA). Tamoxifen was dissolved in ethanol to give a concentration of 85 mg/ml. The tamoxifen solution was dissolved in

peanut oil to a final concentration of 12.75 mg/ml. At 6 wk of age, both *iRAmKO*$^{-}$ and *iRAmKO*$^{+}$ mice were given a 160 μl, i.p. injection of the tamoxifen solution every 24 h for a total of 5 d. Some mice received additional injections of tamoxifen after a surgical procedure (*e.g.*, synergist ablation or myotenectomy). In these instances, the mice were treated with 80 μl/d of the aforementioned tamoxifen solution. The injections were given for 3 consecutive d followed by 1 d off, and then this sequence was repeated for the remainder of the recovery period.

Rapamycin and puromycin injections

Rapamycin was purchased from L. C. Laboratories (Woburn, MA, USA) and was dissolved in DMSO to generate a 5 μg/μl stock solution. For experiments involving maximal-intensity contractions, 1.0 mg/kg rapamycin in 200 μl of PBS was administered *via* an intraperitoneal injection at 100 min before the onset of stimulation. For all other experiments, either 0.6 mg/kg or 1.5 mg/kg of rapamycin in 200 μl of PBS was administered *via* an intraperitoneal injection immediately before initiating a surgical procedure. These injections were repeated every 24 h for up to 14 d. For all control conditions, an equivalent amount of DMSO was administered in 200 μl PBS.

Puromycin was purchased from MilliporeSigma and was dissolved in diH_2O to generate a 75 mM stock solution. For all *in vivo* measurements of protein synthesis, 0.04 μmol/g puromycin in 200 μl of PBS was administered *via* an intraperitoneal injection at exactly 30 min before muscle collection (23).

Measurement of voluntary running

The *iRAmKO*$^{+}$ mice and their control (*iRAmKO*$^{-}$) littermates were individually housed in cages that contained a running wheel equipped with a magnetic counter switch. Running wheel activity was then continuously measured for the next 5 d with Vital View software (Mini-Mitter Company, Bend, OR, USA), and the resulting data was used to calculate the average voluntary distance run per day.

Maximal-intensity contractions

The model previously described by O'Neil *et al.* (24) was used to induce maximal-intensity contractions (MIC) in the tibialis anterior (TA) muscle. Specifically, electrodes were placed on the sciatic nerve of the right leg, and contractions were elicited by stimulating the sciatic nerve with an SD9E Grass Stimulator (Grass Instruments, Quincy, MA, USA) at 100 Hz, 4–8 V pulse, for 10 sets of 6 contractions. Each contraction lasted 3 s and was followed by a 10-s and then a 1-min rest period was provided between each set. Both the right TA and the left TA, which was used as a contralateral control muscle, were collected 1 h after the last set of contractions and subjected to the various treatments described as follows.

Intermittent passive stretch

Mouse extensor digitorum longus (EDL) muscles were subjected to intermittent passive stretch in an *ex vivo* organ culture system that consisted of a refined myograph apparatus (Kent Scientific, Torrington, CT, USA) and an organ culture bath as previously described (25). Briefly, the proximal and distal tendons of muscles were connected to a micromanipulator and the lever arm of a force transducer, respectively. The length of the muscle was adjusted to optimal length, and the muscles were then subjected to intermittent 15% passive stretch for 90 min as a source of mechanical stimulation, or held static at optimal length as a control condition. The bath incubation medium consisted of high glucose DMEM that was maintained at 37°C with continuous 95% O_2 and 5% CO_2 gassing and was exchanged with fresh medium at 30-min intervals (Hyclone; GE Healthcare Life Sciences, Waukesha, WI, USA). For all *ex vivo* measurements of protein synthesis, EDL muscles were incubated in fresh medium containing 2.7 mM phenylalanine and 10 mCi/ml ^{3}H-phenylalanine (PerkinElmer, Waltham, MA, USA) during the final 30 min, and an aliquot of the medium was saved before collecting the muscles to normalize the specific activity of the phenylalanine (cpm/nmol of phenylalanine). The specific activity of the phenylalanine incorporated into the muscle proteins was obtained by using trichloroacetic acid, and the rate of protein synthesis was calculated as previously described (25).

Synergist ablation and myotenectomy

Bilateral synergist ablation surgeries were performed by removing the soleus and distal half of the gastrocnemius muscle as previously described (7). Bilateral myotenectomy surgeries were performed by removing only the distal tendon and myotendinous junction of the gastrocnemius muscle. Mice in the control groups were subjected to a sham surgery where an incision was made on the lower leg and then closed. Following the surgeries, incisions were closed with Vetbond surgical glue and sutures (Henry Schein, Melville, NY, USA). Mice were allowed to recover for 0, 3, 7, or 14 d. During the recovery period, the mice were treated with 1 mg/d tamoxifen for 3 consecutive days followed by 1 d off, and then this sequence was repeated for the remainder of the recovery period. At the end of the recovery period the plantaris muscles were collected and subjected to the various treatments described below. It bears mentioning that we also attempted to examine soleus muscles in the myotenectomy model. However, we discovered that during the course of adapting to myotenectomy, the soleus muscles become rigorously fused with a layer of connective tissue that forms in the lateral space that was previously occupied by the myotendinous junction of the gastrocnemius. Consequently, we were unable to obtain clean and intact dissections of the soleus muscles.

Western blot analysis

Upon collection, muscles were immediately frozen in liquid nitrogen. The samples were homogenized with a Polytron for 20 s in ice-cold buffer A [40 mM Tris (pH 7.5), 1 mM EDTA, 5 mM EGTA, 0.5% Triton X-100, 25 mM β-glycerophosphate, 25 mM NaF, 1 mM Na3VO4, 10 mg/ml leupeptin, and 1 mM PMSF]. Either the whole homogenate was used for further analysis or the homogenate was centrifuged at 2500 *g* for 5 min and then the supernatant was used for further analysis (*e.g.*, Western blots of mTOR). Sample protein concentration was determined with a DC protein assay kit (Bio-Rad, Hercules, CA, USA). Equivalent amounts of protein from each sample were dissolved in Laemmli buffer, heated to 100°C for 5 min, and then subjected to electrophoretic separation by SDS-PAGE. Following electrophoretic separation, proteins were transferred to a PVDF membrane and blocked with 5% powdered milk in TBS containing 0.1% Tween 20 (TBST) for 1 h followed by an overnight incubation at 4°C with primary antibody dissolved in TBST containing 1% bovine serum albumin. After an overnight incubation, the membranes were washed for 30 min in TBST and then probed with a peroxidase-conjugated secondary antibody for 1 h at room temperature. Following 30 min of washing in TBST, the blots were developed on film or with a Chemi410 camera mounted to an Autochemi System (UVP, Upland, CA, USA) using regular ECL reagent (Pierce, Rockford, IL, USA) or ECL Prime reagent (Amersham, Piscataway, NJ, USA). Once the appropriate image was captured, the membranes were stained with Coomassie blue to verify equal

loading in all lanes. Images were quantified using ImageJ software [National Institutes of Health (NIH), Bethesda, MD, USA; *http://rsb.info.nih.gov/nih-image/*].

mTOR, LAMP2, dystrophin, and embryonic myosin heavy chain localization

Tissues were collected and immediately submerged in optimal cutting temperature compound (Tissue-Tek; Sakura Finetek USA, Torrance, CA, USA) at resting length and then frozen in liquid nitrogen-chilled isopentane. Midbelly cross sections (2 μm thick) were taken perpendicular to the long axis of the muscle with a cryostat and immediately fixed in −20°C acetone for 10 min. Sections were warmed to room temperature for 5 min and then incubated in PBS for 15 min, followed by a 1-h incubation in buffer B [0.5% bovine serum albumin, 0.3% CHAPS, and 5% normal goat serum (Jackson ImmunoResearch Laboratories, West Grove, PA, USA)]. After 3–5 min washes in PBS, samples were incubated for 1 h in buffer B containing primary antibodies against mTOR (7C10), the lysosome associated membrane protein 2 (LAMP2), and dystrophin or embryonic myosin heavy chain. After 3–5 min washes with PBS, sections were incubated for 1 h with solution B containing secondary antibodies: DyLight 594-conjugated anti-rabbit IgG (H+L), Alexa Fluor 488-conjugated anti-rat IgG (H+L), and Alexa Fluor 350 anti-mouse IgG1 or Alexa Fluor 488-conjugated anti-mouse IgG1. Finally, sections were washed with PBS, and monochrome fluorescence images were captured with a Nikon DS-QiMc camera (Nikon, Tokyo, Japan) on a Nikon 80i epifluorescence microscope by an investigator that was blinded to the sample identification. The monochrome images were then merged using Nikon NIS-Elements D software. Pearson's correlation coefficients and frequency scatterplots that compared the intensity of the signal for mTOR *vs.* LAMP2 within every pixel of the images were generated with the WCIF ImageJplug-in (*http://www.uhnresearch.ca/facilities/wcif/imagej/*). In some instances, Pearson's correlation coefficients and frequency scatterplots were also generated for specific fiber types within a given image [*e.g.*, the embryonic myosin heavy chain (eMHC) positive fibers]. To generate this information, screens were created in Adobe Photoshop so that only the fibers of interest within a given image were visible. In other analyses, the number of pixels in each image that were intensely positive for both mTOR and LAMP2 was quantified with the ImageJ JACoP plugin (*http://rsbweb.nih.gov/ij/plugins/track/jacop.html*) as previously described (26). Briefly, JACoP was used to determine the number of pixels that exceeded an intensity threshold of 45 relative light units for both mTOR and LAMP2, and these pixels were counted as "intense colocalized pixels." All image analyses were performed by investigators that were blinded to the sample identification.

Muscle fiber type and cross-sectional area

Tissues were immediately submerged in optimal cutting temperature compound (Tissue-Tek) at resting length and then frozen in liquid nitrogen-chilled isopentane. Midbelly cross sections (10 μm thick) were taken perpendicular to the long axis of the muscle with a cryostat and immediately fixed in −20°C acetone for 10 min. Immunohistochemistry for individual fiber types was performed as previously described (27). Images of the entire cross section were captured, and then the cross-sectional area of up to 80 randomly selected fibers of each fiber type (type IIa, IIx, or IIb) were measured by tracing the periphery of the fiber using Nikon NIS-Elements D software. All image analyses were performed by investigators that were blinded to the sample identification.

Antibodies

Primary antibodies, Cox IV (3E11; 4850), Cytochrome C (136F3; 4280), mTOR (2972), mTOR (7C10; 2983), p70 (2708), phospho p70 (389; 9234), raptor (24C12; 2280S), S6 (2217S), phospho S6 (240/4; 5364S), phospho S6 (235/6; 2211), tubulin αβ (2148), 4EBP1 (9644), and phospho 4EBP1(36/45; 2855) were purchased from Cell Signaling Technology (Danvers, MA, USA). Anti-dystrophin (Dy8/6C5) was purchased from Novacastra (Leica Microsystems, Buffalo Grove, IL, USA). Anti-LAMP2 (GL2A7) (ab13524) was purchased from Abcam (Cambridge, MA, USA). Anti-laminin (L9393) was obtained from MilliporeSigma. Anti-puromycin (MABE343) was obtained from MilliporeSigma. Antibodies against embryonic myosin heavy chain (clone F1.652), type IIa myosin heavy chain (clone SC-71), type IIx myosin heavy chain (clone 6H1), and type IIb myosin heavy chain (clone BF-F3) were obtained from the Developmental Studies Hybridoma Bank (University of Iowa, Iowa City, IA, USA). Alexa 488 anti-mouse IgM, μ chain specific (115-545-075), Alexa 488 anti-mouse IgG1 (115-545-205), Alexa 488 anti-rat (112-545-16), DyLight 594 anti-rabbit (111-515-144), and peroxidase-labeled anti-mouse IgG2a (115-035-206) were from Jackson ImmunoResearch Laboratories. Alexa 350 anti-mouse IgG1 (A21120) was from Thermo Fisher Scientific, Waltham, MA, USA. Peroxidase-labeled anti-rabbit (PI-1000) was purchased from Vector Laboratories (Burlingame, CA, USA).

Statistical analysis

Statistical significance was determined by using a Student's *t* test or 2-way ANOVA, followed by a Student–Newman–Keuls *post hoc* analysis. Differences between groups were considered significant when $P \leq 0.05$. All statistical analyses were performed on SigmaPlot/SigmaStat software (Systat Software, San Jose, CA, USA).

RESULTS

Characterization of the skeletal muscle specific and inducible raptor knockout mice

Skeletal muscle specific and tamoxifen inducible raptor knockout mice (*iRAmKO*$^+$), along with control mice (*iRAmKO*$^-$), were generated as described in Materials and Methods. To determine the earliest time point at which a maximal knockout of raptor could be achieved, both strains were treated with 2 mg/d of tamoxifen for 5 d, and then the TA muscles were collected at 7, 14, and 21 d post-tamoxifen dosage. The results indicated that, within 7 d, a significant reduction in the protein levels of both raptor and mTOR (*i.e.*, mTORC1) could be detected in the muscles from *iRAmKO*$^+$ mice, and this reduction reached a maximum within 14–21 d post-tamoxifen dosage (**Fig. 1*A***).

To determine whether the knockout of raptor was specific to skeletal muscle, we measured the protein levels of raptor in various tissues including the soleus muscles, brain, heart, and liver. The outcome of these measurements revealed that the knockout of raptor could only be detected in the skeletal muscles (Supplemental Fig. S1). We also determined that, at 21 d post-tamoxifen (2 mg/d for 5 d), the *iRAmKO*$^+$ mice did not reveal any of the problematic traits that have been described in RAmKO mice (20). For instance, TA muscles from the *iRAmKO*$^+$ mice did not reveal any alterations in markers of mitochondrial content (*e.g.*, Cox IV and cytochrome C), muscle mass, or fiber size (Fig. 1*B–E* and Supplemental Fig. S2). Moreover, the daily voluntary activity, and overall physical appearance, of the *iRAmKO*$^+$ mice was indistinguishable from that

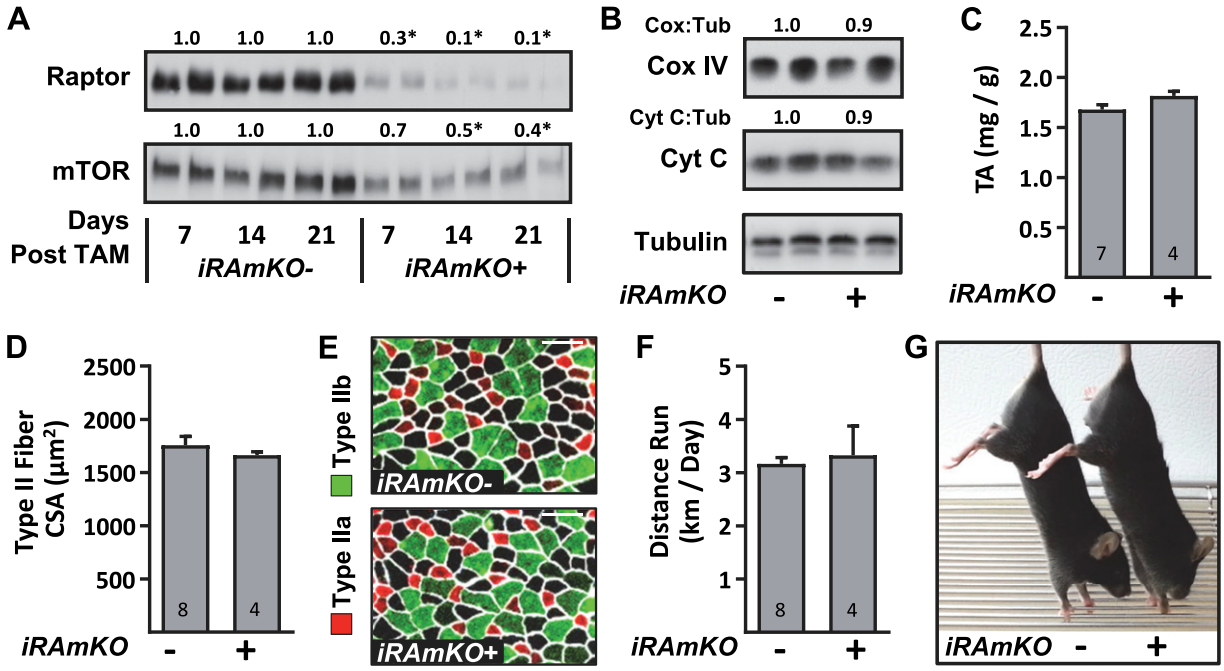

Figure 1. Characterization of skeletal muscle specific and inducible raptor knockout mice. *A*) Skeletal muscle specific and inducible raptor knockout mice (*iRAmKO*$^{+}$), along with control littermates (*iRAmKO*$^{-}$), were treated with 2 mg/d of tamoxifen for 5 d (Tam). At 7, 14, or 21 d post-Tam, TA muscles were collected and subjected to Western blot analysis. Values are expressed relative to the time-matched *iRAmKO*$^{-}$ samples. *B*) Western blot analysis of TA muscles from 21 d post-Tam mice. Values represent the ratios of Cox IV and Cytochrome C (Cyt C) to tubulin (Tub) and are expressed relative to the *iRAmKO*$^{-}$ samples. *C*) Muscle weight to bodyweight ratio of TA muscles at 21 d post-Tam. *D*) Cross-sectional area (CSA) of each fiber type (*i.e.*, type IIa, IIx, and IIb) in the TA muscles at 21 d post-Tam was determined, and then the average of these values was used to calculate the "type II fiber CSA" (individual fiber type data are shown in Supplemental Fig. S2). *E*) Representative images of the cross sections that were stained for laminin (white) as well as type IIa and type IIb fibers. Scale bars, 100 μm. *F*) Average voluntary distance run during a 5-d period in mice that were 17–21 d post-Tam. *G*) Photograph of 21 d post-Tam mice. All values represent the group means + SEM; n = 4–8/group as indicated in the graphs and Supplemental Fig. S11 which contains additional quantitative information. *$P \leq 0.001$, significantly different from the time-matched *iRAmKO*$^{-}$.

of their 21 d post-tamoxifen (2 mg/d for 5 d) *iRAmKO*$^{-}$ (control) littermates (Fig. 1*F*, *G*).

The role of raptor/mTORC1 in the mechanical activation of RSmTOR-dependent signaling

Having established the skeletal muscle specific and inducible raptor knockout model, we next set out to determine whether raptor is necessary for the activation of the RSmTOR-dependent signaling events that are induced by mechanical stimuli. Specifically, we first used a model in which TA muscles were subjected to a bout of MIC *via* electrical stimulation of the sciatic nerve. To date, it has been widely reported that this type of mechanical stimulation induces a robust activation of RSmTOR-dependent signaling events; yet, this has never been directly confirmed (24, 28). Therefore, to establish whether MICs induce the activation of RSmTOR-dependent signaling, we treated wild-type mice with, or without, rapamycin, subjected their TA muscles to a bout of MICs, and then evaluated the muscles for several commonly used markers of RSmTOR-dependent signaling. As shown in **Fig. 2*A***, the results demonstrated that MICs promote an increase in the phosphorylation of the 70 kDa ribosomal S6 kinase (p70) on the threonine 389 residue [P-p70(389)], as well as the ribosomal S6 protein (S6) on the serine 235/236 [P-S6(235/6)] and the serine 240/244 [P-S6 (240/4)] residues, but do not promote an alteration in phosphorylation of the eukaryotic translation initiation factor 4E-binding protein 1 (4EBP1) on the threonine 36/45 residues [P-4EBP1(36/45)]. Furthermore, rapamycin completely abolished the ability of MICs to induce an increase in p70(389) phosphorylation, but it did not prevent MICs from promoting an increase in S6(235/6) or S6(240/4) phosphorylation. Combined, these results indicate that the MIC-induced increase in p70(389), but not S6(235/6) or S6(240/4) phosphorylation, is mediated by a fully rapamycin-sensitive, and presumably mTOR-dependent, mechanism.

Although rapamycin is considered to be a highly specific inhibitor of mTOR, it remained possible that the inhibitory effects of rapamycin were exerted through nonspecific (mTOR-independent) actions. Thus, to address this, we used transgenic mice that possess skeletal muscle specific expression of a rapamycin-resistant mutant of mTOR (RR-mTOR) (7, 25). As shown in Fig. 2*B*, the expression of RR-mTOR rescued the MIC-induced increase in p70(389) phosphorylation from the inhibitory effects of rapamycin. This was an important observation because it confirmed that mTOR is the rapamycin-sensitive element that conferred the MIC-induced increase in p70(389) phosphorylation, and therefore, established that MICs induce a robust activation of RSmTOR-dependent signaling.

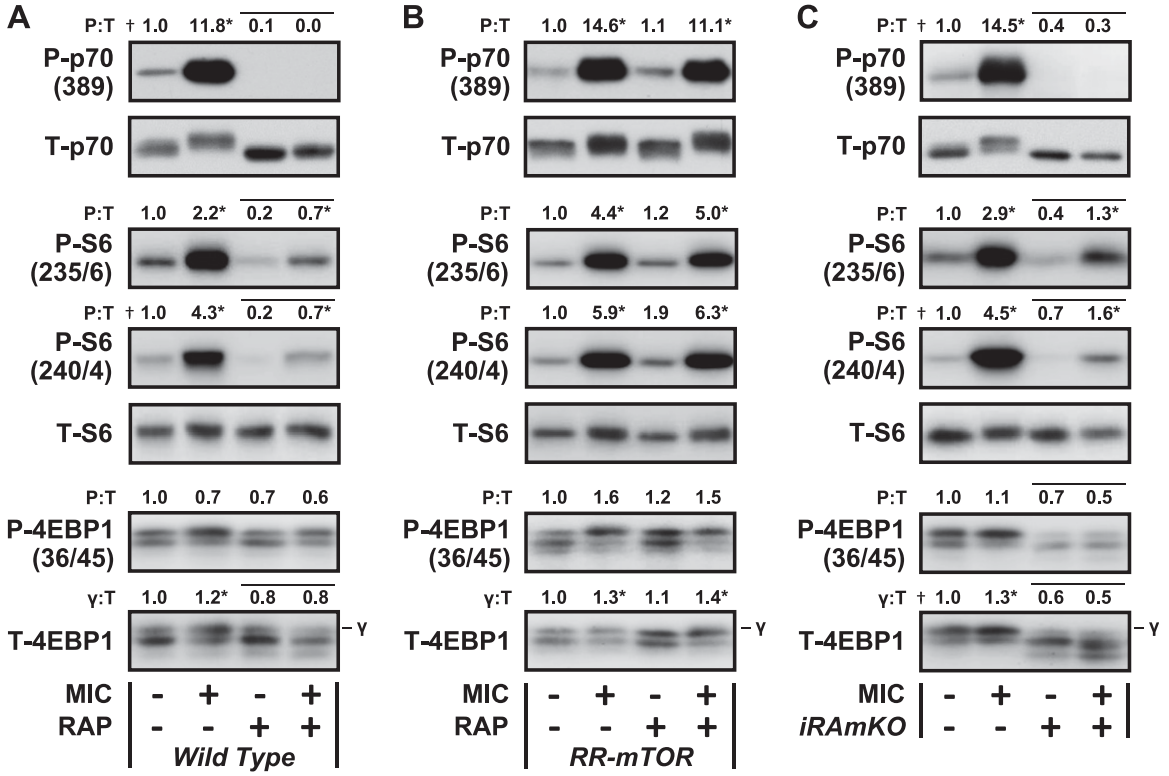

Figure 2. Raptor/mTORC1 is necessary for, at least a subset of, the RSmTOR-dependent signaling events that are activated by maximal-intensity contractions. *A*, *B*) Wild-type FVB (*A*) and FVB (*B*) mice with skeletal muscle specific expression of a rapamycin-resistant mutant of mTOR (RR-mTOR) were treated with rapamycin (RAP^+) or the solvent vehicle (RAP^-), and then the tibialis anterior (TA) muscles were stimulated with a bout of maximal-intensity contractions (MIC^+) or the control condition (MIC^-). At 1 h after stimulation, the TA muscles were collected and subjected to Western blot analysis. Values represent the phosphorylated to total ratio (P:T) expressed relative to the genotype-matched control group (*i.e.*, RAP^- and MIC^-). *C*) At 21 d after being treated with 2 mg/d of tamoxifen for 5 d (Tam), TA muscles from skeletal muscle specific and inducible raptor knockout mice ($iRAmKO^+$), and the control littermates ($iRAmKO^-$), were subjected to a bout of MIC, or the control condition, and then analyzed as previously described. Values represent the group means for the P:T ratios, or the percentage of 4EBP1 in the γ form (γ:T), expressed relative to the control group (*i.e.*, $iRAmKO^-$ and MIC^-); n = 4–6/group. Horizontal bar above the values indicates a main effect for RAP (*A*) or *iRAmKO* (*C*). $^*P < 0.05$, significant effect of MIC within the given level of RAP or *iRAmKO*; $^\dagger P < 0.05$, significant interaction between RAP and MIC (*A*), or *iRAmKO* and MIC (*C*). Additional quantitative information can be found in Supplemental Fig. S11.

In a final set of experiments, we subjected muscles from $iRAmKO^-$ and $iRAmKO^+$ mice to a bout of MICs. Western blot analyses revealed that, like rapamycin, the loss of raptor/mTORC1 significantly reduced S6(235/6) and S6 (240/4) phosphorylation, but it did not prevent MICs from promoting an increase in the phosphorylation of these sites (Fig. 2C). On the other hand, the loss of raptor/mTORC1 completely abolished the ability of MICs to induce an increase in p70(389) phosphorylation. Similar results were also obtained when EDL muscles were subjected to mechanical stimulation *via* an *ex vivo* bout of intermittent passive stretch (Supplemental Fig. S3) (25). Thus, when combined, the results from these analyses indicate that raptor/mTORC1 is necessary for, at least a subset of, the RSmTOR-dependent signaling events that are induced by mechanical stimuli.

Raptor is necessary for the targeting of mTOR to the late endosome/lysosome

Next, we set out to develop a better understanding of why raptor is necessary for the mechanical activation of RSmTOR-dependent signaling. During this effort, we were particularly inspired by previous studies that have suggested that raptor regulates RSmTOR-dependent signaling by controlling the intracellular localization of mTOR (29, 30). This was an attractive concept because work from our laboratory has demonstrated that mTOR is enriched at the late endosomal/lysosomal (LEL) system in skeletal muscle, and that its association with the LEL is further enhanced when muscles are stimulated with a bout of MICs (26). Moreover, previous studies have also demonstrated that, in HEK293T cells, raptor is necessary for the enhanced targeting of mTOR to the LEL that occurs in response to amino acid stimulation (29). Based on these points, we reasoned that raptor might be necessary for the mechanical activation of RSmTOR-dependent signaling because it targets mTOR to the LEL. To begin testing this, we first measured the degree of colocalization between mTOR and LAMP2 (a marker of the LEL) in unstimulated (*i.e.*, control) TA muscles from $iRAmKO^-$ and $iRAmKO^+$ mice. As shown in Supplemental Fig. S4, our results demonstrated that mTOR is highly colocalized with the LEL in muscles from $iRAmKO^-$ mice, and that this pattern

of colocalization was abolished in muscles from *iRAmKO*$^+$ mice. Moreover, as shown in **Fig. 3**, we found that MICs induce a further increase in the colocalization of mTOR with the LEL in muscles from *iRAmKO*$^-$ mice, and again, this effect was abolished in muscles from *iRAmKO*$^+$ mice. Combined, these results establish that raptor is necessary for efficient targeting of mTOR to the LEL in both control and mechanically stimulated muscles.

The synergist ablation model of mechanical overload induces reexpression of raptor in the muscle fibers of *iRAmKO*$^+$ mice

To determine whether raptor is necessary for mechanically induced hypertrophy, we first attempted to use the synergist ablation model of mechanical overload. To date, synergist ablation has been the most widely used rodent model for inducing muscle hypertrophy and defining the underlying mechanisms that regulate this process (31, 32). Synergist ablation involves the surgical removal of the gastrocnemius and soleus muscles, and as a result, the plantaris muscle is subjected to chronic mechanical overload and adapts with a robust hypertrophic response. Importantly, we and others have shown that synergist ablation–induced hypertrophy is completely blocked when mice are treated with rapamycin and that mTOR is the rapamycin-sensitive element that confers the hypertrophic response (6, 7). However, the mechanical stimulus imposed by synergist ablation is highly supraphysiologic, and it induces marked signs of regeneration and/or hyperplasia (*e.g.*, a dramatic increase in the number of eMHC positive fibers) (7). This was a concern because expression of the tamoxifen inducible Cre recombinase in the *iRAmKO*$^+$ mice is controlled by the HSA promoter, a promoter that is not highly expressed in satellite cells (33). Hence, any satellite cell fusion that occurs during regeneration/hyperplasia might result in the formation of muscle fibers that contain satellite cell DNA, and thus, intact copies of the raptor gene. Based on this point, we suspected that it would be very difficult to maintain the knockout of raptor in muscles that were subjected to synergist ablation. Indeed, when we subjected *iRAmKO*$^-$ and *iRAmKO*$^+$ mice to 7 d of synergist ablation, it resulted in a substantial increase in the expression of both raptor and mTOR in the muscles from *iRAmKO*$^+$ mice (**Fig. 4*A***).

To establish whether the increase in raptor was occurring within the muscle fibers, we needed to be able to visualize where raptor is expressed. Unfortunately, however, we were unable to identify an antibody that could be used to visualize raptor with a high degree of specificity in skeletal muscle cross sections. To overcome this, we deferred to the use of an indirect immunohistochemical measurement of raptor expression. Specifically, as shown in Supplemental Fig. S4, we had already determined that raptor is necessary for the targeting of mTOR to the LEL. Thus, we reasoned that if raptor is being reexpressed in muscle fibers of *iRAmKO*$^+$ mice, then this should also induce recolocalization of mTOR with the LEL in these fibers. To test this, *iRAmKO*$^-$ and *iRAmKO*$^+$ mice were subjected to 7 d of synergist ablation, or a sham surgery, and then cross sections of the plantaris muscles were stained for mTOR and LAMP2 (Fig. 4*B*). Colocalization

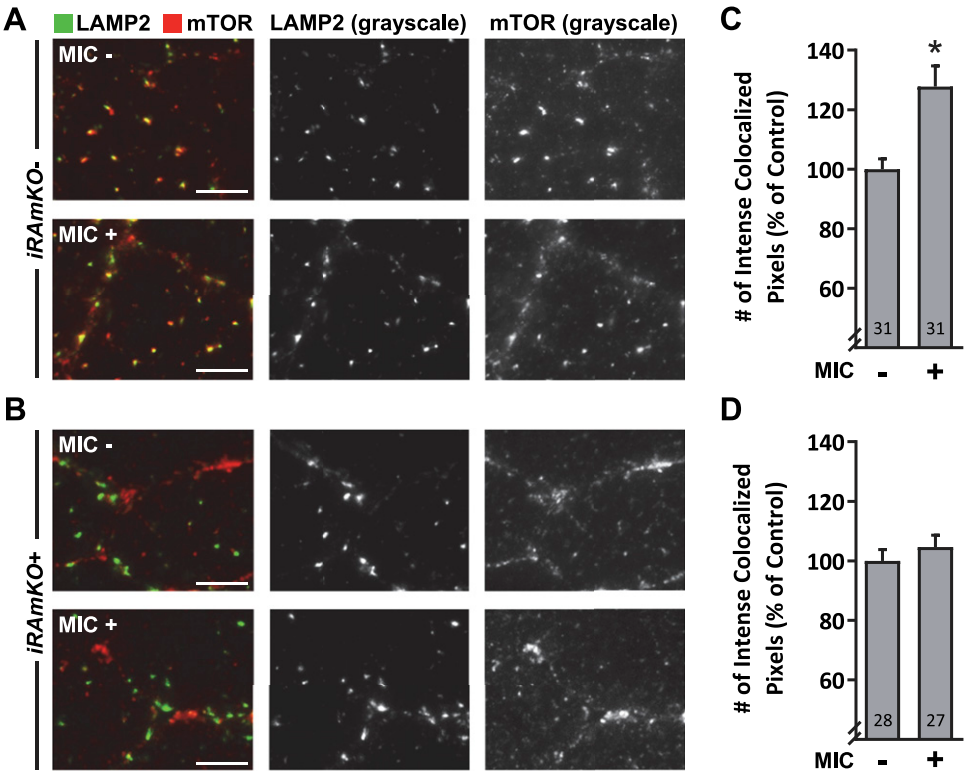

Figure 3. Maximal-intensity contractions enhance the targeting of mTOR to the LEL system *via* a raptor-dependent mechanism. At 21 d after being treated with tamoxifen (2 mg/d for 5 d), the tibialis anterior muscles from skeletal muscle specific and inducible raptor knockout mice (*iRAmKO*$^+$), as well as control littermates (*iRAmKO*$^-$), were stimulated with a bout of maximal-intensity contractions (MIC$^+$) or the control condition (MIC$^-$). At 1 h after stimulation, the muscles were collected and subjected to immunohistochemistry for mTOR and LAMP2 as a marker of the LEL system. *A*, *B*) Representative grayscale and merged images of the signals for mTOR and LAMP2 in muscles from *iRAmKO*$^-$ (*A*) and *iRAmKO*$^+$ (*B*) mice. Scale bars, 10 μm. *C*, *D*) Images from *iRAmKO*$^-$ (*C*), and *iRAmKO*$^+$ (*D*) mice were analyzed for the number of pixels that were intensely positive for both mTOR and LAMP2 (*i.e.*, colocalized), and the results were expressed as a percentage of the mean value obtained in the control samples. All values represent the group means + SEM; n = 27–31 images/group as indicated in graphs. *$P \leq 0.005$, significant effect of MIC.

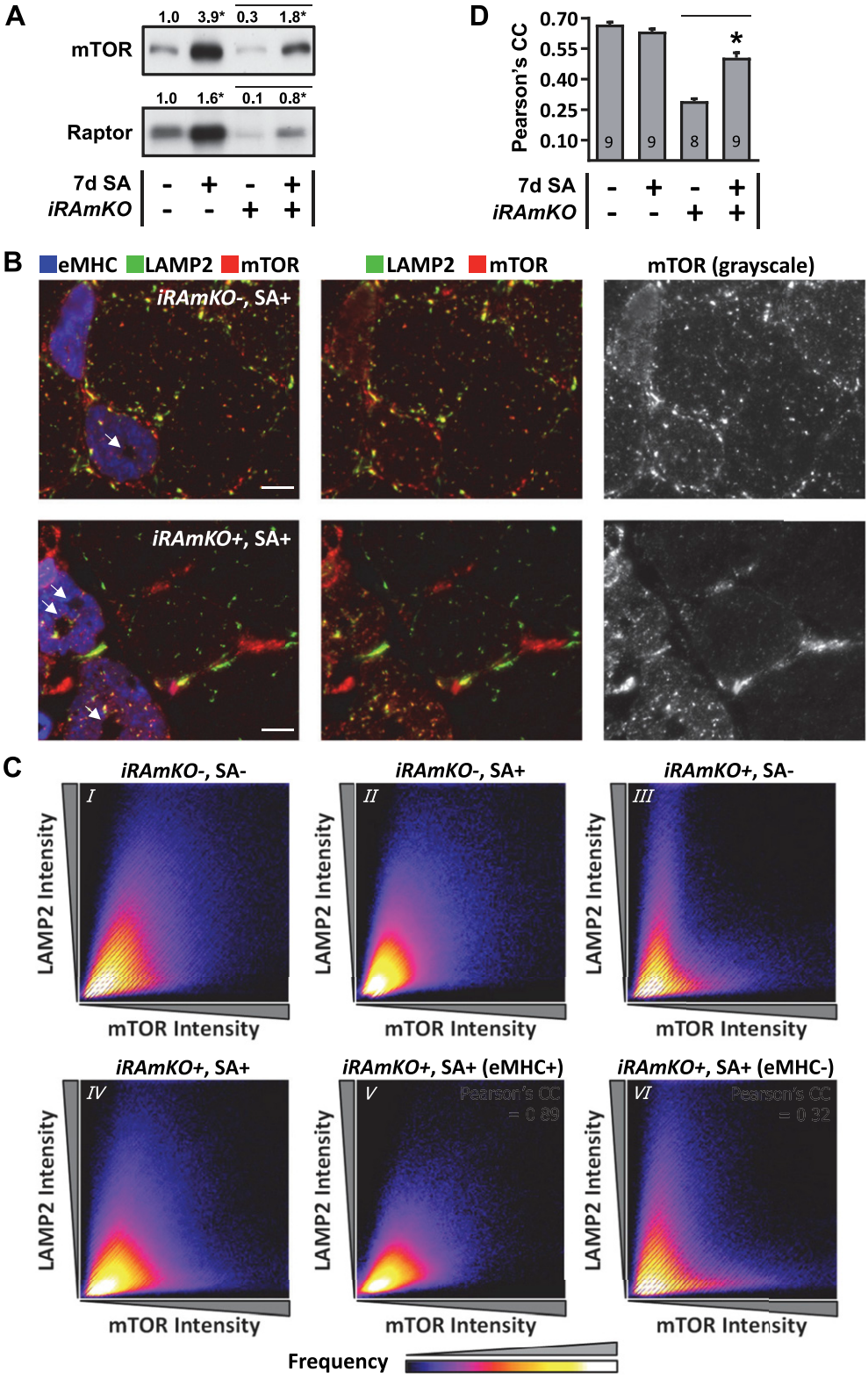

Figure 4. The synergist ablation model of mechanical overload induces reexpression of raptor in the muscle fibers of *iRAmKO*$^{+}$ mice. At 21 d after being treated with tamoxifen (2 mg/d for 5 d), the plantaris muscles from skeletal muscle specific and inducible raptor knockout mice (*iRAmKO*$^{+}$), as well as control littermates (*iRAmKO*$^{-}$), were subjected to synergist ablation (SA^{+}) or a sham (SA^{-}) surgery. During a 7-d recovery period, the mice were treated with daily injections of tamoxifen as detailed in the Materials and Methods, and then the muscles were collected. *A*) Western blot analysis of mTOR and raptor. Values are expressed relative to the control group (*i.e.*, *iRAmKO*$^{-}$ and 7-d SA^{-}). *B–D*) Cross sections of the muscles were subjected to immunohistochemistry for eMHC, mTOR, and LAMP2. *B*) Representative images of the muscles from *iRAmKO*$^{-}$ and *iRAmKO*$^{+}$ mice that had been subjected to SA. Scale bars, 10 μm. *C*) Frequency scatterplots in *I–IV* were generated by comparing the intensity of signal for mTOR *vs.* LAMP2 in every pixel of the analyzed images. Frequency scatterplots in V, VI were generated by only analyzing the pixels within, or outside, of the eMHC positive fibers, respectively. *D*) Pearson's correlation coefficients (CC) between the signals for mTOR and LAMP2. Values represent the group means + SEM in the graph; n = 7-9/group as indicated in the graph and Supplemental Fig. S11 which contains additional quantitative information. Horizontal bar indicates a main effect for *iRAmKO*. *$P \leq 0.001$, significant effect of SA within the given level of *iRAmKO*.

analysis revealed that the loss of colocalization between mTOR and LAMP2 in muscles from *iRAmKO*$^{+}$ mice was significantly restored after 7 d of synergist ablation (Fig. 4*B–D*). This observation indicated that reexpression of raptor was occurring within the muscle fibers. However, upon visual examination, it was clear that this effect did not occur in all muscle fibers, but instead was generally confined to fibers that possessed central core-like structures (see arrowheads in Fig. 4*B*). We suspected that these were regenerated and/or newly formed fibers, and therefore, performed additional analyses in which the cross sections were stained for mTOR, LAMP2, and eMHC. The results indicated that a very strong degree of colocalization existed between mTOR and LAMP2 in the

eMHC positive fibers of *iRAmKO*$^+$ mice (Fig. 4*CV*), while the degree of colocalization between mTOR and LAMP2 in the eMHC negative fibers was not significantly affected by synergist ablation (Fig. 4C, compare III with VI). When taken together, the results from these analyses indicate that, in muscles from *iRAmKO*$^+$ mice, synergist ablation leads to the reexpression of raptor in eMHC positive, but not eMHC negative, fibers.

Myotenectomy is an effective model for mechanical overload-induced hypertrophy and does not induce reexpression of raptor in the muscle fibers of *iRAmKO*$^+$ mice

Because of the large reexpression of raptor in the muscle fibers of *iRAmKO*$^+$ mice, we could not convincingly use the synergist ablation model to define the role of raptor/mTORC1 in mechanical overload-induced hypertrophy. Thus, we developed a new mechanical overload model in which only the distal tendon and the associated myotendinous junction of the gastrocnemius muscle was removed. We refer to this model as myotenectomy, and our initial analyses revealed that, unlike synergist ablation, myotenectomy did not lead to a significant increase in the number of eMHC positive fibers (**Fig. 5*A***). We also determined that 14 d of myotenectomy was able to induce a significant hypertrophic response, and that the hypertrophic response was mediated through a fully rapamycin-sensitive mechanism (Fig. 5*B* and Supplemental Fig. S5). Based on these results, it appeared that myotenectomy could be a suitable model for determining whether raptor is necessary for mechanical overload-induced hypertrophy.

To further examine the potential usefulness of the myotenectomy model, we subjected the plantaris muscles of *iRAmKO*$^-$ and *iRAmKO*$^+$ mice to myotenectomy for various amounts of time and then measured the protein levels of raptor and mTOR. The outcomes revealed that myotenectomy induced a slight but significant increase in the expression of both raptor and mTOR in *iRAmKO*$^+$ mice (Fig. 5*C, D*). However, the magnitude of this effect was much smaller than what was observed in the synergist ablation model, and it was also paralleled by a similar increase in the expression of raptor and mTOR in muscles from *iRAmKO*$^-$ mice (Fig. 5*C, D*). Based on these points, we suspected that the myotenectomy-induced increase in raptor and mTOR might have resulted from the infiltration of nonmuscle cells (*e.g.*, macrophages, neutrophils, *etc.*), rather than from reexpression of these proteins within the *iRAmKO*$^+$ muscle fibers. Therefore, to examine this, we subjected *iRAmKO*$^-$ and *iRAmKO*$^+$ mice to 7 d of myotenectomy, or a sham surgery, and then cross sections of the plantaris muscles were stained for mTOR and LAMP2 as well as dystrophin to identify the periphery of individual muscle fibers (Fig. 5*E*). In stark contrast with what was observed in the muscles of *iRAmKO*$^+$ mice that were subjected to synergist ablation (Fig. 4*D*), myotenectomy did not significantly alter the colocalization of mTOR and LAMP2 (Fig. 5*F*). Moreover, we noticed that myotenectomy led to an increase in the presence of mTOR positive cells that resided outside of the dystrophin boundary, and that this effect was observed in muscles from both *iRAmKO*$^-$ and *iRAmKO*$^+$ mice (Fig. 5*E*). Combined, these observations suggested that the myotenectomy-induced increase in raptor and mTOR expression occurs outside of the muscle fibers and, more importantly, that the knockout of raptor within the muscle fibers of *iRAmKO*$^+$ mice could be effectively maintained during myotenectomy.

Raptor/mTORC1 is necessary for mechanical overload-induced hypertrophy

Having obtained the evidence which indicated that myotenectomy induces hypertrophy through a fully rapamycin-sensitive pathway, and that the knockout of raptor can be effectively maintained during myotenectomy, we next examined whether raptor/mTORC1 is necessary for the hypertrophic effects of myotenectomy. Specifically, *iRAmKO*$^-$ and *iRAmKO*$^+$ mice were subjected to 7 or 14 d of myotenectomy, or a sham surgery, and then cross sections of the muscles were subjected to immunohistochemistry to identify the size of individual fiber types (*e.g.*, type IIa, IIx, and IIb). Interestingly, we found that the knockout of raptor led to a transient increase in the size of the fibers of the sham muscles (Supplemental Figs. S6 and 7). More importantly, myotenectomy led to a progressive hypertrophic response in muscles from *iRAmKO*$^-$ mice, with the largest hypertrophic response occurring in type IIa fibers (58% increase after 14 d) and the smallest increase (27%) occurring in type IIb fibers, and none of these hypertrophic responses were observed in the muscles from *iRAmKO*$^+$ mice (**Fig. 6** and Supplemental Fig. S6). These results indicated that raptor/mTORC1 is necessary for mechanical overload-induced hypertrophy. However, it still remained possible that the loss of the hypertrophic response in the muscles from *iRAmKO*$^+$ mice was not due to the absence of raptor/mTORC1, but instead was due to a nonspecific effect of the HSA-MCM transgene (*i.e.*, the tamoxifen inducible Cre recombinase). Therefore, to address this, nonfloxed HSA-MCM positive mice, and their nonfloxed HSA-MCM negative littermates, were subjected to 14 d of myotenectomy. As shown in Supplemental Fig. S8, the outcomes revealed that the hypertrophic effect of myotenectomy was not altered by the presence of the HSA-MCM transgene. As such, the results from our studies demonstrate that raptor/mTORC1 is necessary for mechanical overload-induced hypertrophy.

Raptor/mTORC1 is not necessary for a mechanical overload-induced increase in protein synthesis

Alterations in skeletal muscle mass are driven by changes in the balance between the rate of protein synthesis and protein degradation, and signaling by mTOR has been widely implicated in the regulation of protein synthesis (34–36). Consistent with this notion, several studies have shown that rapamycin can prevent the initial increase in protein synthesis that occurs in response to various forms of mechanical stimulation (9, 37–39). Accordingly, current models in the field indicate mTORC1 primarily regulates

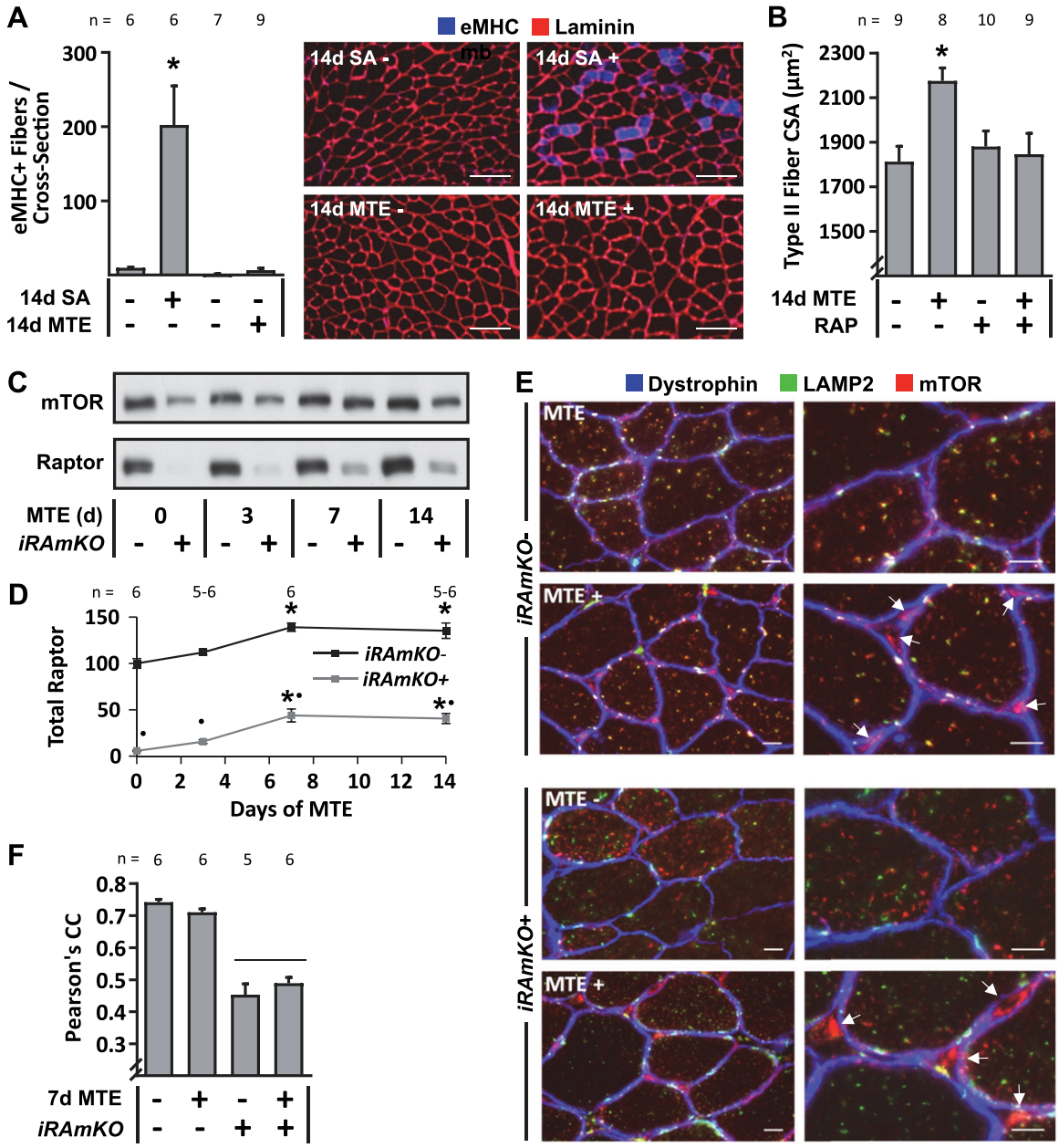

Figure 5. Myotenectomy is an effective model for mechanical overload-induced hypertrophy, and it does not induce the re-expression of raptor in skeletal muscle fibers of *iRAmKO*$^{+}$ mice. *A*) The plantaris (PLT) muscles of wild-type C57BL6 mice were subjected to synergist ablation (SA^{+}), myotenectomy (MTE^{+}), or their respective sham surgeries as a control condition. After 14 d of recovery, cross sections of the PLT muscles were subjected to immunohistochemistry for laminin and eMHC, and then the total number of eMHC-positive fibers in the entire cross section was determined. Scale bars, 100 μm. *B*) The PLT muscles of wild-type C57BL6 mice were subjected to MTE or a sham surgery as the control condition, and then the mice were treated with daily injections of 1.5 mg/kg rapamycin (RAP^{+}) or the solvent vehicle (RAP^{-}). After 14 d of recovery, the PLT muscles were collected and subjected to immunohistochemistry for fiber type identification. The mean CSA of each fiber type (*i.e.*, type IIa, IIx, and IIb) was determined, and then the average of these values was used to calculate the "type II fiber CSA" (individual fiber type data is shown in Supplemental Fig. S5). *C–F*) At 21 d after being treated with tamoxifen (2 mg/d for 5 d), skeletal muscle specific and inducible raptor knockout mice (*iRAmKO*$^{+}$), along with control littermates (*iRAmKO*$^{-}$), were subjected to MTE or a sham surgery, treated with daily injections of tamoxifen as described in Materials and Methods, and then the PLT muscles were collected after a 3-, 7-, or 14-d recovery period. Nonsurgically treated mice were used for a 0 d MTE^{-} condition. *C*) Western blot analysis of mTOR and raptor. *D*) The amount of raptor at each time point was expressed as a percentage of the control condition (*i.e.*, *iRAmKO*$^{-}$ and 0 d MTE^{-}). *E, F*) Muscles from the 7-d time point were subjected to immunohistochemistry for dystrophin, mTOR, and LAMP2. *E*) Representative images for each group with the images on the right revealing a magnified region of the images on the left. Scale bars, 10 μm. Arrows indicate mTOR positive cells that resided outside of the dystrophin boundary. *F*) Pearson's CC between the signal for mTOR and LAMP2. All values represent the group means + SEM in the graph; n = 5-10/group as indicated in the graphs and Supplemental Fig. S11 which contains additional quantitative information. Horizontal bar above the values indicates a main effect for *iRAmKO*. *$P \leq 0.005$, significantly different from the control condition; •$P \leq 0.005$, significantly different from the time-matched *iRAmKO*$^{-}$ group.

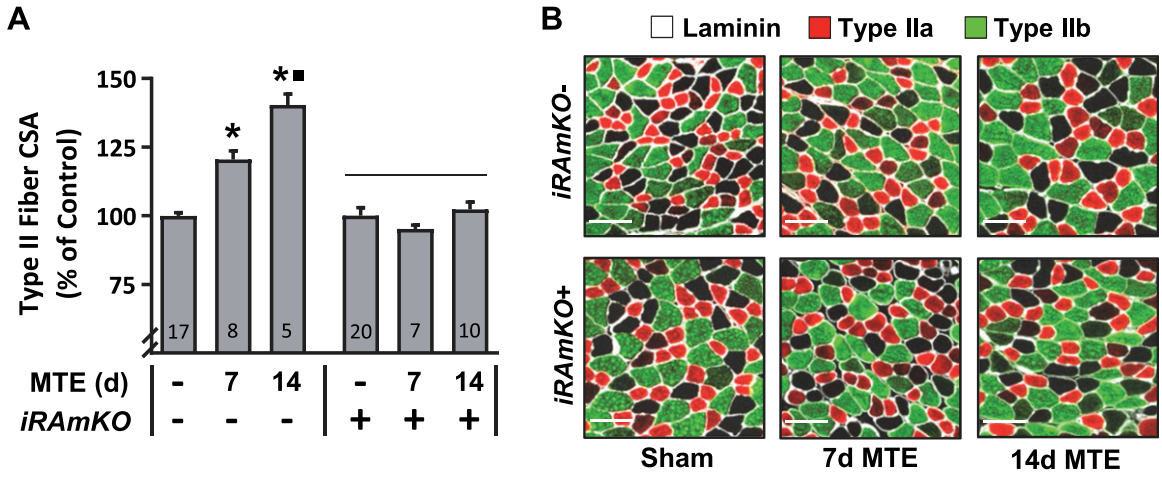

Figure 6. Raptor is necessary for myotenectomy-induced hypertrophy. At 21 d after being treated with tamoxifen (2 mg/d for 5 d), skeletal muscle specific and inducible raptor knockout mice (*iRAmKO*$^{+}$), and control littermates (*iRAmKO*$^{-}$), were subjected to myotenectomy (MTE) or a sham surgery, treated with daily injections of tamoxifen as described in Materials and Methods, and then the plantaris muscles were collected after a 7- or 14-d recovery period. Cross sections were subjected to immunohistochemistry for laminin and fiber type identification. *A*) The mean CSA of each fiber type (*i.e.*, type IIa, IIx, and IIb) was determined, and then the average of these values was used to calculate the "type II fiber CSA." The resulting values were expressed relative to the mean value obtained in the genotype-matched sham group (individual fiber type data is shown in Supplemental Fig. S6). *B*) Representative images of cross sections that were stained for type IIa and type IIb fibers. Scale bars, 100 μm. Values represent the group means + SEM; n = 5–20 muscles/group as indicated in the graph. Horizontal bar indicates a main effect for *iRAmKO*. *$P \leq 0.001$, significant effect of MTE within the given level of *iRAmKO*; ■$P \leq 0.001$, significantly different from the genotype-matched 7-d MTE group.

mechanical overload-induced hypertrophy *via* its ability to promote an increase in the rate of protein synthesis (40–44). Thus, to directly test this notion, *iRAmKO*$^{-}$ and *iRAmKO*$^{+}$ mice were subjected to 7 d of myotenectomy, or a sham surgery, followed by a puromycin injection for the *in vivo* measurement of protein synthesis (23). Surprisingly, the results revealed that, similar to the muscles from control mice, the muscles of *iRAmKO*$^{+}$ mice exhibited a highly robust increase in the rate of protein synthesis (**Fig. 7**). Analogous results were also obtained when EDL muscles from *iRAmKO*$^{-}$ and *iRAmKO*$^{+}$ mice were subjected to an *ex vivo* bout of intermittent passive stretch (Supplemental Fig. S9), as well as when wild-type mice were subjected to synergist ablation and treated with rapamycin (Supplemental Fig. S10). These unexpected results illustrate that mTORC1-/RSmTOR-dependent signaling events are not necessary for a mechanical overload-induced increase in protein synthesis, and the potential implications of this finding will be further addressed in the discussion.

DISCUSSION

Work from several independent laboratories have established that RSmTOR-dependent signaling events play a critical role in the pathway through which mechanical stimuli regulate skeletal muscle mass (6–9). Moreover, numerous reports have shown that a subset of mTORC1-dependent, but not mTORC2-dependent, signaling events are highly sensitive to inhibition by rapamycin (10, 11). Based on this point, it has been widely assumed that mTORC1 is responsible for the RSmTOR-dependent

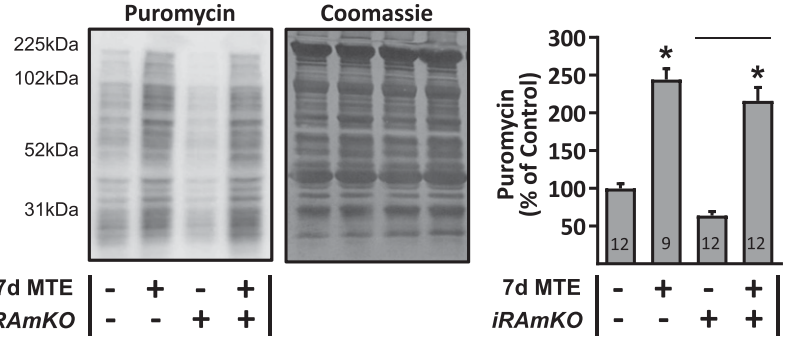

Figure 7. Raptor/mTORC1 is not necessary for a mechanical overload-induced increase in protein synthesis. At 21 d after being treated with tamoxifen (2 mg/d for 5 d), skeletal muscle specific and inducible raptor knockout mice (*iRAmKO*$^{+}$), and control littermates (*iRAmKO*$^{-}$), were subjected to MTE or a sham surgery, and then treated with daily injections of tamoxifen during a 7-d recovery period. At 30 min before collection, the mice were injected with puromycin, and then the plantaris muscles were subjected to Western blot analysis to quantify the amount of puromycin-labeled peptides (*i.e.*, the rate of protein synthesis). The membranes were also stained with Coomassie to verify equal loading of protein in all lanes. Values in the graph are expressed relative to the control group (*i.e.*, *iRAmKO*$^{-}$ and MTE^{-}) and represent the group means ± SEM; n = 9–12/group as indicated in the graph. Horizontal bar above the values indicates a main effect for *iRAmKO*. *$P \leq 0.01$, significant effect of MTE within the given level of *iRAmKO*.

signaling events that are evoked by mechanical stimuli. However, as mentioned in the introduction, a growing body of evidence has raised concerns about this assumption. Thus, the first major question we addressed in this study was whether raptor/mTORC1 is necessary for the RSmTOR-dependent signaling events that are induced by mechanical stimuli. To address this, we treated mice with or without rapamycin, subjected their muscles to a bout of MICs as a source of mechanical stimulation, and then analyzed the muscles for markers of RSmTOR-dependent signaling. The outcomes revealed that MICs induce a robust increase in p70(389) phosphorylation and that this event is mediated through a fully rapamycin-sensitive mechanism. Next, by using mice that express a rapamycin-resistant mutant of mTOR, we were able to verify that mTOR is the rapamycin-sensitive element that confers the MIC-induced increase in p70(389) phosphorylation. Finally, we subjected muscles from *iRAmKO*$^{-}$ and *iRAmKO*$^{+}$ mice to a bout of MICs and found that raptor/mTORC1 is necessary for the MIC-induced increase p70(389) phosphorylation. Similar results were also observed when muscles were subjected to intermittent passive stretch as a source of mechanical stimulation (Supplemental Fig. S3). Thus, when taken together, 3 important conclusions can be drawn from our analyses: *1*) mechanical stimuli induce a robust activation of RSmTOR-/mTORC1-dependent signaling; *2*) changes in p70(389) phosphorylation are a valid marker for the mechanical activation of RSmTOR-/mTORC1-dependent signaling; and *3*) mTORC1 is necessary for, at least a subset of, the RSmTOR-dependent signaling events that are induced by mechanical stimuli. In addition to making these conclusions, we also determined that raptor is necessary for the targeting of mTOR to the LEL, and this observation likely explains why raptor is necessary for the mechanical activation of mTORC1 signaling [for additional details on this concept see Jacobs *et al*. (45)].

Although MICs induced a robust increase in p70(389) phosphorylation, they did not induce an alteration in 4EBP1(36/45) phosphorylation. This was an intriguing observation because an extensive number of studies have shown that classic agonists of RSmTOR-dependent signaling (*e.g.*, growth factors and nutrients) induce an increase in both p70(389) and 4EBP1(36/45) phosphorylation and that this effect is mediated through a raptor/mTORC1-dependent mechanism (46–48). So why did MICs induce a robust increase in p70(389) phosphorylation while having no effect on 4EBP1(36/45) phosphorylation? According to the study by Kang et al. (11), various mTORC1 regulated phosphorylation sites possess different capacities to serve as substrates for mTORC1 (*i.e.*, substrate quality) which, in turn, determines their sensitivity to physiologic modulators of mTORC1 activity. For example, 4EBP1(36/45) has been described as a very good substrate for mTORC1, and this renders it rapamycin-resistant, but still raptor-dependent. By contrast, other phosphorylation sites such as p70(389) and the serine 64 residue on 4EBP1 [4EBP1(64)] have been described as poor substrates for mTORC1 and, consequently, they are highly sensitive to the inhibitory effects of rapamycin (11). Accordingly, we propose that the unstimulated muscles already possessed a very high level of 4EBP1(36/45) phosphorylation, and therefore, the MIC-induced activation of mTORC1 was unable to induce a further increase in 4EBP1(36/45) phosphorylation. On the other hand, because p70(389) is a poor substrate for mTORC1, the unstimulated muscles would have had a low level of p70 (389) phosphorylation, and therefore, p70(389) was able to undergo a dramatic increase in phosphorylation when mTORC1 became activated. We suspect that a similar type of event would have happened with 4EBP1(64) phosphorylation. If correct, this would explain why MICs induced an increase in the percentage of the γ (*i.e.*, hyperphosphorylated) form of 4EBP1 despite no changes in 4EBP1(36/45) phosphorylation (Fig. 2).

The next major question we wanted to address in this study was whether signaling by raptor/mTORC1 is necessary for mechanical overload-induced hypertrophy. To address this, we used a skeletal muscle specific and inducible knockout based approach because, as explained in the introduction, the constitutive knockout of raptor in skeletal muscle results in a number of problematic traits. Of note, current skeletal muscle specific and inducible knockout approaches rely on the use of promoters that are expressed in mature muscle fibers (*e.g.*, the HSA or MCK promoter), but these promoters are not highly expressed in satellite cells (22, 33, 49). This is a noteworthy point because mechanical overload can cause satellite cells to fuse with the pre-existing, regenerating, and/or newly forming muscle fibers (50), and thus, introduce intact alleles of the genes that were previously knocked out. Indeed, we obtained evidence which indicated that the synergist ablation model of chronic mechanical overload led to the reexpression of raptor within muscle fibers that stained positive for eMHC. Thus, to overcome this, we developed the myotenctomy model, which, as shown in Fig. 5, induced hypertrophy through a rapamycin-sensitive mechanism but did not lead to the appearance of eMHC positive fibers or any indications that reexpression of raptor had occurred within the fibers. These were important milestones because they helped to establish that the myotenectomy model, in conjunction with the skeletal muscle specific and inducible knockout based approach, could be used to determine whether raptor (and effectively any gene of interest) is necessary for mechanical overload-induced hypertrophy.

As shown in Fig. 6, our results with the myotenectomy model revealed that raptor/mTORC1 is necessary for mechanical overload-induced hypertrophy. Unexpectedly, however, we also discovered that raptor/mTORC1 is not necessary for a mechanical overload-induced increase in protein synthesis (Fig. 7). This was a surprising observation because previous studies have reported that rapamycin can inhibit the increase in protein synthesis that occurs in response to various forms of mechanical stimulation (9, 37–39), and thus, it has been widely assumed that the activation of RSmTOR/mTORC1 regulates mechanical overload-induced hypertrophy *via* its ability to promote an increase in the rate of protein synthesis (40–44). Therefore, to further confirm our findings, we performed a complementary experiment in which wild-type mice were subjected to synergist ablation and then treated with, or without, rapamycin. Consistent with our findings in the *iRAmKO*$^{+}$ mice, the outcomes

revealed that rapamycin does not prevent the synergist ablation-induced increase in protein synthesis (Supplemental Fig. S10). Thus, it can be concluded that RSmTOR-/mTORC1-dependent signaling events are not required for a mechanical overload-induced increase in the rate of protein synthesis.

Although the aforementioned outcomes were unexpected, they are highly congruent with recent studies in rats which have shown that rapamycin does not completely prevent the increase in protein synthesis that occurs at later time points following a bout of electrically evoked contractions (8, 51, 52). Interestingly, Ogasawara and Suginohara (52) have shown that this rapamycin-insensitive increase in protein synthesis can be completely abolished when signaling by both mTORC1 and mTORC2 are blocked with the mTOR kinase inhibitor AZD8055. Thus, it appears that signaling by rapamycin-insensitive mTORC2 might contribute to the mechanical overload-induced increase in protein synthesis, and this topic will certainly be worthy of further investigation.

Based on our results, we have concluded that signaling through RSmTOR/mTORC1 is necessary for mechanical overload-induced hypertrophy, but it is not required for a mechanical overload-induced increase in protein synthesis. So then why is signaling through an RSmTOR-/mTORC1-dependent mechanism necessary for a hypertrophic response? Currently, the answer to this question is not known, but there are at least 2 possibilities that are worthy of consideration. First, a recent study by Marabita et al. found that, during Akt-induced skeletal muscle hypertrophy, the knockout of p70 (a classic RSmTOR-/mTORC1-dependent target that regulates protein synthesis) attenuated the hypertrophic response, but it did not attenuate the Akt-induced increase in the rate of protein synthesis. This study also revealed that, in the absence of p70, the activation of Akt led to the accumulation of p62-positive protein aggregates (53). This is noteworthy because the presence of p62-positive protein aggregates is often due to the accumulation of mistranslated and/or misfolded proteins (54, 55). Hence, the regulation of p70 by RSmTOR/mTORC1 might play a role in controlling the quality of newly synthesized proteins. If correct, then in the absence of RSmTOR-/mTORC1-dependent signaling, a normal increase in the rate of protein synthesis might be evoked by mechanical overload, but a significant portion of these newly synthesized proteins would not be properly translated/processed, and therefore, would not contribute to a hypertrophic response. A second point to consider is the role of RSmTOR-/mTORC1-dependent signaling in the regulation of autophagy. Specifically, it is well known that the activation of RSmTOR-/mTORC1-dependent signaling suppresses autophagy (56). Thus, in the absence of RSmTOR-/mTORC1-dependent signaling, mechanical overload would presumably lead to a robust increase in autophagy and, in turn, counteract the increase in protein synthesis that would normally drive a hypertrophic response. It will be of great importance for future studies to address these possibilities and to develop a more comprehensive understanding of the basic mechanisms through which RSmTOR/mTORC1 regulates mechanical overload-induced hypertrophy. FJ

ACKNOWLEDGMENTS

This research was supported by the U.S. National Institutes of Health, National Institute of Arthritis and Musculoskeletal and Skin Diseases Grant AR057347 (to T.A.H.). The authors declare no conflicts of interest.

AUTHOR CONTRIBUTIONS

J.-S. You, R. M. McNally, B. L. Jacobs, and T. A. Hornberger designed the experiments; J.-S. You, R. M. McNally, and T. A. Hornberger wrote the manuscript; and all authors acquired and analyzed data.

REFERENCES

1. Seguin, R., and Nelson, M. E. (2003) The benefits of strength training for older adults. *Am. J. Prev. Med.* **25**(3, Suppl 2)141–149
2. Janssen, I., Shepard, D. S., Katzmarzyk, P. T., and Roubenoff, R. (2004) The healthcare costs of sarcopenia in the United States. *J. Am. Geriatr. Soc.* **52**, 80–85
3. Pahor, M., and Kritchevsky, S. (1998) Research hypotheses on muscle wasting, aging, loss of function and disability. *J. Nutr. Health Aging* **2**, 97–100
4. Bodine, S. C. (2013) Disuse-induced muscle wasting. *Int. J. Biochem. Cell Biol.* **45**, 2200–2208
5. Adams, G. R., and Bamman, M. M. (2012) Characterization and regulation of mechanical loading-induced compensatory muscle hypertrophy. *Compr. Physiol.* **2**, 2829–2870
6. Bodine, S. C., Stitt, T. N., Gonzalez, M., Kline, W. O., Stover, G. L., Bauerlein, R., Zlotchenko, E., Scrimgeour, A., Lawrence, J. C., Glass, D. J., and Yancopoulos, G. D. (2001) Akt/mTOR pathway is a crucial regulator of skeletal muscle hypertrophy and can prevent muscle atrophy *in vivo*. *Nat. Cell Biol.* **3**, 1014–1019
7. Goodman, C. A., Frey, J. W., Mabrey, D. M., Jacobs, B. L., Lincoln, H. C., You, J. S., and Hornberger, T. A. (2011) The role of skeletal muscle mTOR in the regulation of mechanical load-induced growth. *J. Physiol.* **589**, 5485–5501
8. Ogasawara, R., Fujita, S., Hornberger, T. A., Kitaoka, Y., Makanae, Y., Nakazato, K., and Naokata, I. (2016) The role of mTOR signalling in the regulation of skeletal muscle mass in a rodent model of resistance exercise. *Sci. Rep.* **6**, 31142
9. Drummond, M. J., Fry, C. S., Glynn, E. L., Dreyer, H. C., Dhanani, S., Timmerman, K. L., Volpi, E., and Rasmussen, B. B. (2009) Rapamycin administration in humans blocks the contraction-induced increase in skeletal muscle protein synthesis. *J. Physiol.* **587**, 1535–1546
10. Zhou, H., and Huang, S. (2010) The complexes of mammalian target of rapamycin. *Curr. Protein Pept. Sci.* **11**, 409–424
11. Kang, S. A., Pacold, M. E., Cervantes, C. L., Lim, D., Lou, H. J., Ottina, K., Gray, N. S., Turk, B. E., Yaffe, M. B., and Sabatini, D. M. (2013) mTORC1 phosphorylation sites encode their sensitivity to starvation and rapamycin. *Science* **341**, 1236566
12. Ikenoue, T., Hong, S., and Inoki, K. (2009) Monitoring mammalian target of rapamycin (mTOR) activity. *Methods Enzymol.* **452**, 165–180
13. Pasiakos, S. M. (2012) Exercise and amino acid anabolic cell signaling and the regulation of skeletal muscle mass. *Nutrients* **4**, 740–758
14. Yamada, A. K., Verlengia, R., and Bueno Junior, C. R. (2012) Mechanotransduction pathways in skeletal muscle hypertrophy. *J. Recept. Signal Transduct. Res.* **32**, 42–44
15. Patursky-Polischuk, I., Stolovich-Rain, M., Hausner-Hanochi, M., Kasir, J., Cybulski, N., Avruch, J., Rüegg, M. A., Hall, M. N., and Meyuhas, O. (2009) The TSC-mTOR pathway mediates translational activation of TOP mRNAs by insulin largely in a raptor- or rictor-independent manner. *Mol. Cell. Biol.* **29**, 640–649
16. Ge, Y., and Chen, J. (2012) Mammalian target of rapamycin (mTOR) signaling network in skeletal myogenesis. *J. Biol. Chem.* **287**, 43928–43935
17. You, J. S., Lincoln, H. C., Kim, C. R., Frey, J. W., Goodman, C. A., Zhong, X. P., and Hornberger, T. A. (2014) The role of diacylglycerol kinase ζ and phosphatidic acid in the mechanical activation of mammalian target of rapamycin (mTOR) signaling and skeletal muscle hypertrophy. *J. Biol. Chem.* **289**, 1551–1563

18. Yip, C. K., Murata, K., Walz, T., Sabatini, D. M., and Kang, S. A. (2010) Structure of the human mTOR complex I and its implications for rapamycin inhibition. *Mol. Cell* **38**, 768–774
19. Bentzinger, C. F., Lin, S., Romanino, K., Castets, P., Guridi, M., Summermatter, S., Handschin, C., Tintignac, L. A., Hall, M. N., and Rüegg, M. A. (2013) Differential response of skeletal muscles to mTORC1 signaling during atrophy and hypertrophy. *Skelet. Muscle* **3**, 6
20. Bentzinger, C. F., Romanino, K., Cloëtta, D., Lin, S., Mascarenhas, J. B., Oliveri, F., Xia, J., Casanova, E., Costa, C. F., Brink, M., Zorzato, F., Hall, M. N., and Rüegg, M. A. (2008) Skeletal muscle-specific ablation of raptor, but not of rictor, causes metabolic changes and results in muscle dystrophy. *Cell Metab.* **8**, 411–424
21. Sengupta, S., Peterson, T. R., Laplante, M., Oh, S., and Sabatini, D. M. (2010) mTORC1 controls fasting-induced ketogenesis and its modulation by ageing. *Nature* **468**, 1100–1104
22. McCarthy, J. J., Srikuea, R., Kirby, T. J., Peterson, C. A., and Esser, K. A. (2012) Inducible Cre transgenic mouse strain for skeletal muscle-specific gene targeting. *Skelet. Muscle* **2**, 8
23. Goodman, C. A., Mabrey, D. M., Frey, J. W., Miu, M. H., Schmidt, E. K., Pierre, P., and Hornberger, T.A. (2011) Novel insights into the regulation of skeletal muscle protein synthesis as revealed by a new nonradioactive in vivo technique. *FASEB* **25**, 1028–1039
24. O'Neil, T. K., Duffy, L. R., Frey, J. W., and Hornberger, T. A. (2009) The role of phosphoinositide 3-kinase and phosphatidic acid in the regulation of mammalian target of rapamycin following eccentric contractions. *J. Physiol.* **587**, 3691–3701
25. You, J. S., Frey, J. W., and Hornberger, T. A. (2012) Mechanical stimulation induces mTOR signaling via an ERK-independent mechanism: implications for a direct activation of mTOR by phosphatidic acid. *PLoS One* **7**, e47258
26. Jacobs, B. L., You, J. S., Frey, J. W., Goodman, C. A., Gundermann, D. M., and Hornberger, T. A. (2013) Eccentric contractions increase the phosphorylation of tuberous sclerosis complex-2 (TSC2) and alter the targeting of TSC2 and the mechanistic target of rapamycin to the lysosome. *J. Physiol.* **591**, 4611–4620
27. Goodman, C. A., Kotecki, J. A., Jacobs, B. L., and Hornberger, T. A. (2012) Muscle fiber type-dependent differences in the regulation of protein synthesis. *PLoS One* **7**, e37890
28. Gordon, B. S., Steiner, J. L., Lang, C. H., Jefferson, L. S., and Kimball, S. R. (2014) Reduced REDD1 expression contributes to activation of mTORC1 following electrically induced muscle contraction. *Am. J. Physiol. Endocrinol. Metab.* **307**, E703–E711
29. Sancak, Y., Peterson, T. R., Shaul, Y. D., Lindquist, R. A., Thoreen, C. C., Bar-Peled, L., and Sabatini, D. M. (2008) The Rag GTPases bind raptor and mediate amino acid signaling to mTORC1. *Science* **320**, 1496–1501
30. Sancak, Y., Bar-Peled, L., Zoncu, R., Markhard, A. L., Nada, S., and Sabatini, D. M. (2010) Ragulator-Rag complex targets mTORC1 to the lysosomal surface and is necessary for its activation by amino acids. *Cell* **141**, 290–303
31. Terena, S. M., Fernandes, K. P., Bussadori, S. K., Deana, A. M., and Mesquita-Ferrari, R. A. (2017) Systematic review of the synergist muscle ablation model for compensatory hypertrophy. *Rev. Assoc. Med. Bras. (1992)* **63**, 164—172
32. Kirby, T. J., McCarthy, J. J., Peterson, C. A., and Fry, C. S. (2016) Synergist ablation as a rodent model to study satellite cell dynamics in adult skeletal muscle. *Methods Mol. Biol.* **1460**, 43–52 armsscdasm
33. Cox, R. D., Garner, I.,and Buckingham, M. E. (1990) Transcriptional regulation of actin and myosin genes during differentiation of a mouse muscle cell line. *Differentiation* **43**, 183—191
34. Goodman, C. A., Mayhew, D. L., and Hornberger, T. A. (2011) Recent progress toward understanding the molecular mechanisms that regulate skeletal muscle mass. *Cell. Signal.* **23**, 1896–1906
35. Thoreen, C. C., Chantranupong, L., Keys, H. R., Wang, T., Gray, N. S., and Sabatini, D. M. (2012) A unifying model for mTORC1-mediated regulation of mRNA translation. *Nature* **485**, 109–113
36. You, J. S., Dooley, M. S., Kim, C. R., Kim, E. J., Xu, W., Goodman, C. A., and Hornberger, T. A. (2018) A DGKζ-FoxO-ubiquitin proteolytic axis controls fiber size during skeletal muscle remodeling. *Sci. Signal.* **11**, eaao6847
37. Gundermann, D. M., Walker, D. K., Reidy, P. T., Borack, M. S., Dickinson, J. M., Volpi, E., and Rasmussen, B. B. (2014) Activation of mTORC1 signaling and protein synthesis in human muscle following blood flow restriction exercise is inhibited by rapamycin. *Am J Physiol Endocrinol Metab.* **306**, E1198-1204
38. Hornberger, T. A., Stuppard, R., Conley, K. E., Fedele, M. J., Fiorotto, M. L., Chin, E. R., and Esser, K. A. (2004) Mechanical stimuli regulate rapamycin-sensitive signalling by a phosphoinositide 3-kinase-, protein kinase B- and growth factor-independent mechanism. *Biochem. J.* **380**, 795–804
39. Kubica, N., Bolster, D. R., Farrell, P. A., Kimball, S. R., and Jefferson, L. S. (2005) Resistance exercise increases muscle protein synthesis and translation of eukaryotic initiation factor 2Bepsilon mRNA in a mammalian target of rapamycin-dependent manner. *J. Biol. Chem.* **280**, 7570–7580
40. Goodman, C. A. (2014) The role of mTORC1 in regulating protein synthesis and skeletal muscle mass in response to various mechanical stimuli. *Rev. Physiol. Biochem. Pharmacol.* **166**, 43–95
41. Astratenkova, I. V., and Rogozkin, V. A. (2014) [Molecular mechanisms of skeletal muscle hypertrophy]. *Ross. Fiziol. Zh. Im. I M Sechenova* **100**, 649–669
42. Marcotte, G. R., West, D. W., and Baar, K. (2015) The molecular basis for load-induced skeletal muscle hypertrophy. *Calcif. Tissue Int.* **96**, 196–210
43. Spangenburg, E. E. (2009) Changes in muscle mass with mechanical load: possible cellular mechanisms. *Appl. Physiol. Nutr. Metab.* **34**, 328–335
44. Miyazaki, M.,and Esser, K. A. (2009) Cellular mechanisms regulating protein synthesis and skeletal muscle hypertrophy in animals. *J Appl Physiol (1985)* **106**, 1367—1373
45. Jacobs, B. L., Goodman, C. A., and Hornberger, T. A. (2014) The mechanical activation of mTOR signaling: an emerging role for late endosome/lysosomal targeting. *J. Muscle Res. Cell Motil.* **35**, 11–21
46. Yoon, M. S., Du, G., Backer, J. M., Frohman, M. A., and Chen, J. (2011) Class III PI-3-kinase activates phospholipase D in an amino acid-sensing mTORC1 pathway. *J. Cell Biol.* **195**, 435–447
47. Yonezawa, K., Yoshino, K. I., Tokunaga, C., and Hara, K. (2004) Kinase activities associated with mTOR. *Curr. Top. Microbiol. Immunol.* **279**, 271–282
48. Saxton, R. A., and Sabatini, D. M. (2017) mTOR signalings in growth, metabolismgm, and diseased. *Cell* **169**, 361–371
49. Bi, P., Yue, F., Sato, Y., Wirbisky, S., Liu, W., Shan, T., Wen, Y., Zhou, D., Freeman, J., and Kuang, S. (2016) Stage-specific effects of Notch activation during skeletal myogenesis. *eLife* **5**, e17355
50. Murach, K. A., Fry, C. S., Kirby, T. J., Jackson, J. R., Lee, J. D., White, S. H., Dupont-Versteegden, E. E., McCarthy, J. J., and Peterson, C. A. (2018) Starring or supporting role? Satellite cell and skeletal muscle fiber size regulations. *Physiology (Bethesda)* **33**, 26–38
51. West, D. W., Baehr, L. M., Marcotte, G. R., Chason, C. M., Tolento, L., Gomes, A. V., Bodine, S. C., and Baar, K. (2016) Acute resistance exercise activates rapamycin-sensitive and -insensitive mechanisms that control translational activity and capacity in skeletal muscle. *J. Physiol.* **594**, 453–468
52. Ogasawara, R., and Suginohara, T. (2018) Rapamycin-insensitive mechanistic target of rapamycin regulates basal and resistance exercise-induced muscle protein synthesis. *FASEB J.* **32**, 5824–5834
53. Marabita, M., Baraldo, M., Solagna, F., Ceelen, J. J. M., Sartori, R., Nolte, H., Nemazanyy, I., Pyronnet, S., Kruger, M., Pende, M., and Blaauw, B. (2016) S6K1 is required for increasing skeletal muscle force during hypertrophy. *Cell Reports* **17**, 501–513
54. Pankiv, S., Clausen, T. H., Lamark, T., Brech, A., Bruun, J. A., Outzen, H., Øvervatn, A., Bjørkøy, G., and Johansen, T. (2007) p62/SQSTM1 binds directly to Atg8/LC3 to facilitate degradation of ubiquitinated protein aggregates by autophagy. *J. Biol. Chem.* **282**, 24131–24145
55. Ciechanover, A., and Kwon, Y. T. (2015) Degradation of misfolded proteins in neurodegenerative diseases: therapeutic targets and strategies. *Exp. Mol. Med.* **47**, e147
56. Jung, C. H., Ro, S. H., Cao, J., Otto, N. M., and Kim, D. H. (2010) mTOR regulation of autophagy. *FEBS Lett.* **584**, 1287–1295

Received for publication August 15, 2018.
Accepted for publication November 5, 2018.